# “Theoretical and experimental study of Aegle Marmelos leaves extract as eco-friendly anticorrosion agent for Aluminium in HCl”

**V. R. Patel**
**Department of Chemistry,**
**C. B. Patel Computer College and J. N. M. Patel Science College,**
**Surat-395017, Gujarat, India.**

**D. M. Patel**
**Department of Chemistry,**
**C. B. Patel Computer College and J. N. M. Patel Science College,**
**Surat-395017, Gujarat, India.**

**B. M. Patel**
**Department of Chemistry,**
**C. B. Patel Computer College and J. N. M. Patel Science College,**
**Surat-395017, Gujarat, India.**

**N. I. Prajapati**
**Department of Chemistry,**
**C. B. Patel Computer College and J. N. M. Patel Science College,**
**Surat-395017, Gujarat, India.**

**K. K. Patel**
**Department of Chemistry,**
**Shri Govind Guru University, Godhra-388713, Gujarat, India.**

**S. A. Desai**
**Department of Chemistry,**
**C. B. Patel Computer College and J. N. M. Patel Science College,**
**Surat-395017, Gujarat, India.**

## Abstract:

This study explored the corrosion inhibiting properties of Aegle Marmelos (Bael) leaves extract (AMLE) as an eco-friendly solution for aluminium in 0.2 N to 0.6 N Hydrochloric acid solutions. The effectiveness of AMLE was evaluated through gravimetric analysis, potentiodynamic polarization (PDP) and electrochemical impedance spectroscopy (EIS), supported by molecular dynamics (MD) simulations and density functional theory (DFT). The highest inhibition efficiency reached 92.43 % at 4.0 g/dL in 0.2 N HCl. Thermodynamic parameters indicated that adsorption follows Langmuir isotherm. PDP showing a reduction in corrosion current density 143.0 μA/cm² and 20.5 μA/cm² at without and with higher AMLE inhibitor concentration, with EIS confirmed an 85.66 % efficiency. Surface analysis using SEM and EDX provided insights into surface protection and inhibitor interaction. Quantum chemical studies revealed stable adsorption behavior, supporting AMLE's potential as a sustainable, eco-friendly alternative to synthetic corrosion inhibitors for aluminium in acidic environments.

## 1. Introduction:

Metal materials are gradual deterioration by chemical or electrochemical process with its surrounding environment. Aluminium (Al) is commonly used in various industries due to its versatility, conductivity and malleability. Aluminium is used in electronics due to it is super purity[1]. The use of hydrochloric acid and sulphuric acid as a pickling agent or in various cleaning processes contributes to the exacerbation of corrosion related problems. Aluminium has a natural oxide layer that protects it from corrosion. When Aluminium is exposed in corrosive media, the oxide layer is damaged and exposed the metal surface area to the attack of the corrosive environment[2]. Different kinds of inhibitors including organic, inorganic and polymer compounds are used for prevention of metal corrosion, which are often used to coatings, paints or directly applied on the surface of metal[3], but these compounds are very high toxic and hazardous to environment. The search for safe and effective alternative source as corrosion inhibitors lead to the development of natural products of plant origin as corrosion inhibitors.

Recently, some plant extracts as green corrosion inhibitor such as Pomegranate peel[4] ethanol extract prepared by the soxhlet process, effectively inhibition efficiency (I.E.) 92.58% at 3.0 g/L for Al in HNO3 solution investigated using by weight loss, potentiodynamic polarization (PDP), surface morphology by scanning electron microscope (SEM), atomic force microscope (AFM) and contact angle images. Gas chromatography-mass spectrometer (GC-MS) analysis, fourier transform Infrared spectroscopy (FTIR), ultraviolet radiation (UV-IR) and theoretical approach of adsorption study of inhibitor molecule by density functional theory

(DFT) a quantum chemical study of electronic structure and its adsorption properties, Molecular dynamics (MD) simulation a computational study to understand the dynamic behaviour of atoms and molecules on metal surface. Musa paradisiaca stem sap extract[5] using n-hexane solvent in a Soxhlet apparatus found 90.73% I.E. at 20 V/V% inhibitor concentration used gravimetric analysis and electrochemical impedance spectroscopy, Surface analysis was conducted using atomic force microscopy, adsorption stuied by langmuir, temkin, frumkin and freundlich isotherms and Gas chromatograph-Molecular spectra confirmed present of long-chain alkanes, phthalic acid esters and fluorinated compounds in inhibtior form protective barrier on Al in HCl. Yellow oleander[6] flower of dichloromethane extract investigated by mass loss, electrochemical frequency modulation, electrochemical impedance spectroscopy and surface analysis studied using scanning electron microscopy, found maximum 88.70% I.E. at 300 ppm inhibitor concentration for Al in HCl.

Hibiscus sabdariffa leaf[7] ethanolic extract found 95.1% I.E. at 3000 mg/dm3 for Al in HCl investigated by gravimetric tests, electrochemical techniques, Electrochemical techniques included potentiodynamic polarization curves and electrochemical impedance spectroscopy. Xanthium spinosum[8] of dichloromethane extract found 93.1% I.E. at 300 ppm for Al in HCl studied by gravimetric analysis, potentiodynamic polarization, electrochemical impedance spectroscopy, electrochemical frequency modulation spectroscopy and surface morphology by atomic force microscopy and X-ray photoelectron spectroscopy. These are biodegradable, non-toxic easily available and low cost, are being developed for various industrial applications. Green inhibitor contains essential elements like Oxygen, Carbon, Nitrogen and Sulphur heteroatoms and electron-donating groups. The order of inhibition efficiency should be P > S > N > O[9]. The active components in plant extract help in the adsorption of these compounds on Aluminium creating a protective film that protects the surface and hinders corrosion.

Recent research has shown various plant extracts can serve as effective corrosion inhibitors due to their ability to form protective films on metal surfaces[10]. This study investigates the corrosion inhibition action of the aqueous extract of Aegle Marmelos leaves extract (AMLE) in 0.2, 0.4 and 0.6 N hydrochloric acid solution have been investigated using gravimetric method at room temperature and high temperature, kinetic study, adsorption behaviour, potentiodynamic polarization (PDP) electrochemical impedance spectroscopy (EIS), surface morphology by scanning electron microscope (SEM), energy dispersive x-ray spectroscopy (EDX) and theoretical approach of quantum study by density functional theory (DFT) and molecular dynamic (MD) simulation. Thermodynamic analysis provides insight

into the adsorption mechanisms of the plant extract on the Aluminium surface, evaluating parameters such as adsorption free energy and enthalpy. Kinetic studies allow for the determination of corrosion rate changes in the presence of the inhibitor, revealing how it affects the reaction dynamics[11]. DFT analysis offers a molecular-level understanding of the interaction between the active components of the extract and the metal surface, facilitating the identification of key functional groups responsible for corrosion inhibition[12,13]. Aegle marmelos leaves known as Bili patra, Bael patra or Bilva patra is leaf of Bael tree commonly found in tropical regions. It is offering to lord shiva in Hinduism. It is a perennial plant recognized for its rich phytochemical profile and potential medicinal properties. Some researcher found Aegle marmelos leaves contained various phytochemical such as aegelin, lupeol, rutin, marmesinin, γ-sitosterol, β-sitosterol, flavone, glycoside, marmeline and phenylethyl cinnamamides. Aegle marmelos leaves powder contained a rich source of crude fibre; the aqueous extract of leaves contains major phytochemicals such as alkaloids (Aegeline), Flavonoids (Quercetin), etc. that contribute to its pharmacological activities[14-17]; these molecular structures show in fig. 01. By harnessing the corrosion-inhibiting properties of Aegle marmelos leaves in this study investigated for the development of green inhibitors that align with environmental preservation goals[18].

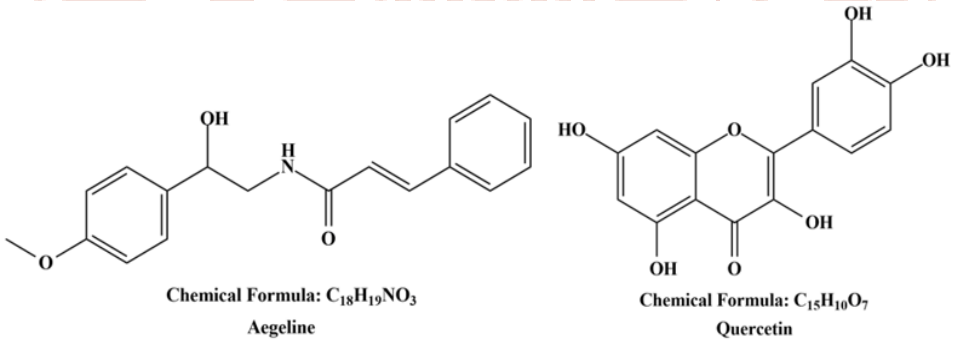


**Fig. 1: Structure of major phytochemical constituents of *AMLE*.**

## 2. Material and Method

### 2.1 Sample preparation:

Aluminium specimens containing 99.28% Al, 0.47% Fe, 0.14% Cu and 0.11% Zn were used in this study. The size of test specimens was 4.96 x 2.49 x 0.2 cm3 with 0.496 cm diameter hole having a total working area of 0.2733 dm2 was used. It was washed with double distilled water, dried and weighted by using electronic balance. 0.2 N, 0.4 N and 0.6 N concentrated corrosive solutions were prepared from A. R. grade HCl purchased from Loba chem pvt. ltd. using double distilled water.

### 2.2 Preparation of inhibitor extract:

The intact Aegle marmelos leaves (Fig. 02) were collected from the waste of shiv temple and local market, clean, washed with distilled water, dried under sunlight and ground

into fine powder. 20 gm of the sample was refluxed in 200 ml distilled water for 2 h, filtered and made up to 100 ml using double distilled water. 1.0, 2.0, 3.0 and 4.0 g/dL concentrations of AMLE solutions were prepare from this stock solution.

**Fig. 02: Aegle Marmelos Leaves.**

**2.3 Gravimetric analysis:**

The experimental solution consisted of different HCl concentration with varying concentrations of inhibitors. The specimens were immersed in the experimental solution using glass hooks. The initial weight of the samples was recorded before keeping them completely immersed in the solution for 24 h at room temperature. After the immersion period, the specimens were removed, washed with distilled water, dried completely and their final weights were measured. The corrosion rate and inhibition efficiency was calculated by equations (01) and (02).

$$\text{Corossion Rate } (\text{mg/dm}^2\text{d}) = \frac{\text{Weight loss (g)} \times 1000}{\text{Area in dm}^2 \times \text{Day}} \quad \ldots (01)$$

$$\text{Inhibtion Efficiency } (\%) = \frac{\text{Wu} - \text{Wi}}{\text{Wu}} \times 100 \quad \ldots (02)$$

Where, Wu = Weight loss of Uninhibited metal and Wi = Weight loss of Inhibited metal

**2.4 Temperature effect:**

The Aluminium samples were absolutely immersed in 200 ml solution having concentration of 0.2 N HCl, without and with various concentrations of AMLE, at different temperatures of 313, 323 and 333K for the duration of 2 h. Activation energy (Ea) was evaluated from the slope of the log(ρ) versus 1/T graph as well as by applying the Arrhenius equation (Equation 03)[19].

$$\log \frac{\rho_1}{\rho_2} = \frac{E_a}{2.303\,R} \log \left[\frac{1}{T_1} - \frac{1}{T_2}\right] \quad \ldots (03)$$

Where, $\rho_1$ and $\rho_2$ are the corrosion rate at $T_1$ and $T_2$ Temperature respectively.

The thermodynamic aspects like Gibbs adsorption energy[20], enthalpy and entropy[21] were calculated using the following equations (04, 05 and 06).

$$G^{\circ}_{ads} = -RT \ln[55.5\, K_{ads}] \quad \ldots (04)$$

$$\Delta H^{\circ}_{ads} = E_{ads} - RT \quad \ldots (05)$$

$$\Delta S^{\circ}_{ads} = [\Delta H^{\circ}_{ads} - \Delta G^{\circ}_{ads}]/T \quad \ldots (06)$$

Where, R is a gas constant in kJ/mol, T is a temperature, Kads is equilibrium constant for adsorption and 55.5 represents the molar concentration of water in the solution.

**2.5 Adsorption isotherm:**

The value of heat of adsorption ($Q_{ads}$) was obtained by the following equation (07)[22].

$$Q_{ads} = 2.303\ R\left[Log\left(\frac{\theta_2}{1-\theta_2}\right) - Log\left(\frac{\theta_1}{1-\theta_1}\right)\right] \times \left[\frac{1}{T_1} - \frac{1}{T_2}\right] \quad \ldots (07)$$

Where, $\theta_1$ and $\theta_2$ were calculated using the formula $\theta = (W_u - W_i)/W_i$ at temperature $T_1$ and $T_2$, where $\theta$ represent the fractions of metal surface coverage by the inhibitor.

**2.6 Electrochemical analysis:**

In the potentiodynamic polarization (PDP) study, a working electrode composed of aluminium, a platinum electrode and a silver/silver chloride (Ag/AgCl) electrode used as the reference electrode. The working electrode as similar Al-alloy has been an exposed surface area of approximately 1 cm². The PDP curves were then obtained by linearly sweeping the electrode potential. These experiments were conducted at in 200 mL of 0.2 N HCl solution without and with 4.0g/dL AMLE concentrations while maintaining a constant temperature of 301 ± 1 K. The polarization data were carefully analysed to determine important corrosion parameters such as the anodic (βa) and cathodic Tafel slopes (βc), polarization resistance (Rp), corrosion potential (Ecorr) and corrosion current density (icorr). An AC voltage with a small amplitude of 5.0 mV, exhibiting sinusoidal variation was applied over a wide frequency spectrum ranging from 1 Hz to 100 kHz. The resulting data were displayed using Nyquist plots, which depict the real part of impedance (Z') versus the imaginary part (Z''). The charge transfer resistance (Rct) and the double-layer capacitance (Cdl) were determined from this plot.

**2.7 Surface morphology:**

Surface analysis was performed using polished 1.0 cm2 of Al specimen, prepared by immersed in a 0.2 N hydrochloric acid (HCl) solution, both without and with of AMLE, for a maximum concentration of 4.0 g/dL for 24 hours at 301 ± 1 K. After immersion, the specimens were removed, air-dried and analysed surface using scanning electron microscopy (SEM) combined with energy-dispersive X-ray spectroscopy (EDX). The analysis was conducted at an accelerating voltage of 10.0 kV and a magnification of 1000X, using Thermofisher scios-2 instrument.

**2.8 Density functional theory (DFT):**

The Density functional theory calculations were performed using the Gaussian 09w software package. The B3LYP functional combined with a 6-31+G(d,p) basis set without and with of water as a solvent, was utilized to assess quantum chemical properties, specifically using Koopman's theorem[23,24]. The analysis included determining the Lowest Unoccupied Molecular Orbital (LUMO) and the Highest Occupied Molecular Orbital (HOMO). Frontier Molecular Orbital Analysis, the energies of the Electron affinity and Ionization potential of the inhibitor molecules will be calculated. The HOMO energy is related to the molecule's ability to donate electrons to the metal surface, while the LUMO energy indicates its ability to accept electrons from the metal surface. The significance of these orbitals reflected in the expression

of ionization potential (I), electron affinity (A), energy difference between the HOMO and LUMO (ΔE), Absolute electronegativity (χ), Global hardness (η) and Electrophilicity index (ω), electron accepting power (ω+), electron donating power (ω-) and nucleophilicity index (ε) derived as indicators of reactivity by following equations[25, 26] (08 to 17).

$A = -HOMO$ … (08)
$I = -LUMO$ … (09)
$\Delta E = I - A$ … (10)
$\chi = I + A / 2$ … (11)
$\eta = I - A / 2$ … (12)
$\sigma = 1 / \eta$ … (13)
$\omega = \chi^2 / 2\eta$ … (14)
$\varepsilon = 1 / \omega$ … (15)
$\omega+ = (I + 3A)^2 / 16(I - A)$ … (16)
$\omega- = (3I + A)^2 / 16(I - A)$ … (17)

The dipole moment (μ) was calculated in Debye units using methods outlined[27]. The change in electron density (ΔN) due to the interaction between inhibitor molecules and Al surface was evaluated based on the relationship defined from the equation (17).

$$\Delta N = \frac{(\chi_{Al} - \chi_{inh})}{2(\eta_{Al} - \eta_{inh})} \quad \text{… (18)}$$

here, "χAl, χinh, ηAl and ηinh" are the electronegativity and hardness values for the inhibitor molecules and Aluminium, respectively. χAl is 1.61 eV, while ηAl equals zero according of the Pauling scale[28]. A positive value of ΔN shows inhibition of metal electron transfer.

The dipole moment (μ) calculated, higher dipole moment is often associated with stronger interactions with the metal surface[29]. Potential adsorption sites on the inhibitor molecules will be identified based on the distribution of electron density and Mulliken charges. The atoms with higher negative charges are more likely to interact with the positively charged Al surface. The ability of AMLE receive and shared electric charge has been determined the electron accepting (ω+) and donating (ω-) power[30].

**2.9 Molecular Dynamics (MD) Simulations:**

MD simulations performed to investigate the adsorption behaviour of the inhibitor molecules on the Al surface in Material studio 2020 software from BIOVIA. The approach of Metropolis Monte Carlo[31], the adsorption locator module was used to enumerate the low energy configuration of inhibitor molecules such as Aegeline and Quercetin. A Monte cralo simulation box (40.49Å x 28.63Å x 32.88Å) were employed including a model Al cleave surface Al(110) with 14 Å thickness, 275 water molecules, 2 Hydronium ions, 2 Chloride ions to represent the HCl solution environment and inhibitor molecule. MD simulation were run COMPASS III force field, applying an energy convergence tolerance of 1 × 10–4 kcal/mol as

well as a force convergence tolerance of 0.005 kcal/molÅ[32]. The diffusion coefficients of the inhibitor molecules, water molecules, hydronium ions and chloride ions were calculated to understand the dynamics of these species at the interface. The adsorption mode and the molecular orientation of inhibitor on Al surface were analysed. The interaction energy between the inhibitor molecules and the Al surface were calculated. This was estimated by analysing the energies of the inhibitor-metal interactions within the simulation.

## 3. Result and discussion:

### 3.1 Gravimetric analysis:

#### 3.1.1 Effect of acid concentration:

The corrosion behaviour of Al was investigate without and with inhibitor in 200ml of 0.2, 0.4 and 0.6N of HCl solution at 301 ± 1 K. Al specimen was immersed in corrosive medium for 24 h immersion period. The rate of corrosion increases as 1653.86, 2747.90 and 3980.97 mg/dm2d with increasing acid concentration at 301 ± 1 K. Al specimen was immersed in 0.2 N HCl solution as corrosive medium at 313, 323 and 333 K temperature. The rate of corrosion increases as 6234.91, 8474.20 and 10889.13 mg/dm2d with increasing temperature.

#### 3.1.2 Effect of inhibitor concentration:

Al specimen were immersed in different concentration of HCl solution with varying concentration as 1.0, 2.0, 3.0 and 4.0 g/dL of AMLE for an immersion period of 24 h at 301±1K. Table 01 shows the maximum I.E. found 92.43%, 80.03% and 69.29% at constant acid concentration as 0.2, 0.4 and 0.6 N respectively. Fig. 03 indicate the addition of the inhibitor significantly reduces the corrosion rate at constant acid concentration and decrease in corrosion rate of Al in HCl solution with increasing concentration of AMLE is primarily attributed to the formation of a protective film on the metal surface.

**Table 01: Inhibition Efficiency (I.E.) and Corrosion Rate (C.R.) of *AMLE* on Al in 0.2 N, 0.4 N and 0.6 N HCl solution for an immersion period of 24 h at 301 ± 1 K.**

| Inhibitor | Inhibitor concentration g/dL | Acid Concentration (HCl) | | | | | |
|---|---|---|---|---|---|---|---|
| | | 0.2 N | | 0.4 N | | 0.6 N | |
| | | C.R. (mg/dm$^2$d) | I.E. (%) | C.R. (mg/dm$^2$d) | I.E. (%) | C.R. (mg/dm$^2$d) | I.E. (%) |
| **Blank** | 0.0 | 1653.86 | - | 2747.90 | - | 3980.97 | - |
| ***AMLE*** | 1.0 | 398.79 | 75.89 | 1375.78 | 49.93 | 2387.12 | 40.04 |
| | 2.0 | 269.67 | 83.69 | 1207.46 | 56.06 | 2089.65 | 47.51 |
| | 3.0 | 183.68 | 88.89 | 863.52 | 68.58 | 1618.73 | 59.34 |
| | 4.0 | 125.14 | 92.43 | 548.85 | 80.03 | 1222.47 | 69.29 |

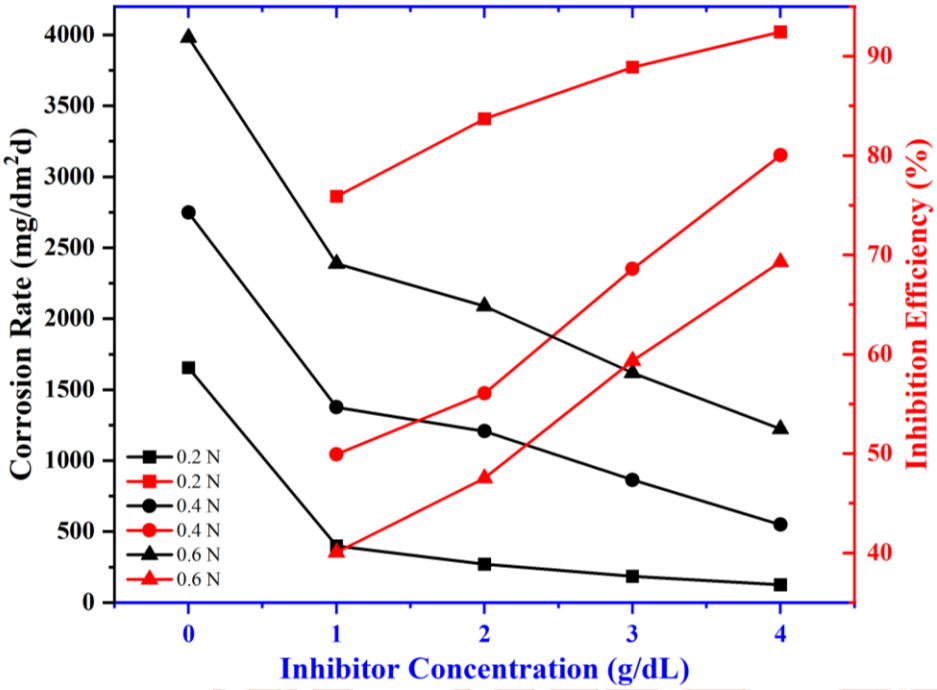


**Fig. 03: Corrosion Rate and Inhibition Efficiency of Al in HCl solution in without and with *AMLE* for an immersion period of 24 h at 301 ± 1 K.**

### 3.2 Effect of temperature:

This study investigated the effects of different temperatures as 313, 323 and 333 K on the corrosion inhibition of Al in 0.2 N HCl solution using various concentrations of inhibitors for 2 h immersion period. Table 02 the results showed that the corrosion rate of Al increased as 6234.91, 8474.20 and 10889.13 mg/dm2d with increasing temperature, while the I.E. decreased. At 4.0 g/dL concentration of AMLE, the I.E. was decreased from 82.39% at 313 K to 59.17% at 333 K.

As temperature rises, the kinetic energy of the molecules involved in the corrosion process increases. This can enhance the rate at which corrosion reactions occur, as higher temperatures generally accelerate the movement of ions in the electrolyte and the diffusion of reactants to the surface of metal. Higher temperatures can lead to an increase in the concentration of aggressive ions (such as $Cl^-$) in certain environments, which can further enhance the corrosion rate. Desorption of certain absorbed molecules could vary with temperature, leading to a decreased concentration of inhibitor at the surface of metal when temperatures are high[33]. As the temperature increases, the corrosion rate of Al typically rises due to enhanced kinetic activity, which can lead to faster electrochemical reactions and a decrease in the effectiveness of inhibitors[34].

**Table 02: Temperature effect on corrosion rate (C.R.), activation energy (Ea) and heat of adsorption (Qads) for Al in 0.2 N HCl solution without and with of AMLE for an immersion period of 2 h.**

| Inhibitor | Inhibitor concen-tration (g/dL) | Temperature (K) | | | | | | Mean $E_a$ (kJ/mol) | Arhenius Plot $E_a$ (kJ/mol) | $Q_{ads}$ (kJ/mol) | |
|---|---|---|---|---|---|---|---|---|---|---|---|
| | | 313 K | | 323 K | | 333 K | | | | | |
| | | C.R. (mg/dm$^2$d) | I.E. (%) | C.R. (mg/dm$^2$d) | I.E. (%) | C.R. (mg/dm$^2$d) | I.E. (%) | | | 313-323 (K) | 323-333 (K) |
| **Blank** | 0.0 | 6234.91 | - | 8474.20 | - | 10889.13 | - | 24.10 | 24.18 | - | - |
| ***AMLE*** | 1.0 | 2283.21 | 63.38 | 3995.61 | 52.85 | 6673.98 | 38.71 | 46.44 | 46.49 | -36.52 | -54.31 |
| | 2.0 | 1756.31 | 71.83 | 3380.90 | 60.10 | 5883.64 | 45.97 | 52.27 | 52.42 | -44.25 | -76.58 |
| | 3.0 | 1448.96 | 76.76 | 2722.28 | 67.88 | 5225.03 | 52.02 | 55.63 | 55.56 | -37.56 | -101.71 |
| | 4.0 | 1097.69 | 82.39 | 2151.48 | 74.61 | 4302.96 | 60.48 | 59.25 | 59.17 | -39.12 | -124.07 |

### 3.3 Energy activation:

Arrhenius plots obtained by equation 03 for the corrosion of Al in 0.2 N HCl solution in presence and absence of different concentration of AMLE shows in fig. 04. The Ea values for the inhibited acids ranged from 46.49 to 59.25 kJ/mol, which was higher than the Ea value of the uninhibited acid (24.10 kJ/mol). As well as the Ea value from Arrhenius plot for inhibited acid range from 46.49 to 59.17 kJ/mol, higher than uninhibited acid (24.18 kJ/mol) shown in table 02. This data present that the inhibitor undergoes physical absorption on the metal surface and this increases the activation energy of the absorption process[35].

The values of Qads were negative ranging from -36.52 to -124.07 kJ/mol which indicate that the adsorption process and consequently the I.E. decreases as the temperature increases, which supports the physisorption mechanism[36].

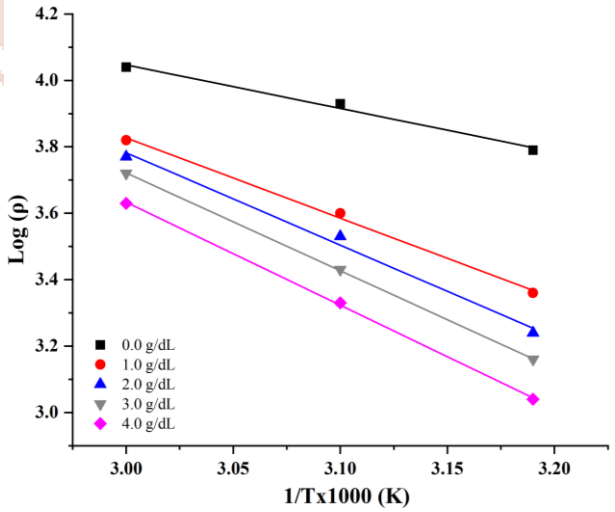


**Fig. 04: Arrhenius plots for corrosion rate of Al in 0.2 N HCl solution without and with of AMLE.**

### 3.4 Adsorption isotherm:

The adsorption of inhibitors on the Al surface is described by the Langmuir adsorption isotherms. Langmuir isotherm suggests that adsorption occurs at specific sites on the metal surface, where each site can hold only one molecule of the inhibitor. This model assumes a homogeneous distribution of binding sites and no interaction between adsorbed molecules[37]. It has been utilized these models to explain the adsorption behaviour of various inhibitors in acidic media. Table 03 shows the value of surface coverage (θ) and C/θ of Langmuir adsorption isotherm represent by the equation (19). A graph of the inhibitor concentration C (g/dL) verses C/θ (Fig. 05) gives a straight line, indicating that the system follows the Langmuir adsorption isotherm[38].

$$\frac{C}{\theta} = \frac{1}{Kads} + C \qquad \ldots (19)$$

Where, Kads is the equilibrium constant and C is inhibitor concentration.

The inhibitor molecules are absorbed on the surface, blocking the reaction sites and thus reducing the corrosion rate.

**Table 03: Surface coverage (θ) of *AMLE* on Al in 0.2 N HCl solution at 301 ± 1 K.**

| Inhibitor | Inhibitor concentration (C) g/dL | Acid Concentration (HCl) | | | | | |
|---|---|---|---|---|---|---|---|
| | | 0.2 N | | 0.4 N | | 0.6 N | |
| | | Surface coverage (θ) | C/θ | Surface coverage (θ) | C/θ | Surface coverage (θ) | C/θ |
| *AMLE* | 1.0 | 0.759 | 1.318 | 0.499 | 2.103 | 0.400 | 2.598 |
| | 2.0 | 0.837 | 2.390 | 0.561 | 3.468 | 0.475 | 4.12 |
| | 3.0 | 0.889 | 3.375 | 0.686 | 4.375 | 0.593 | 5.056 |
| | 4.0 | 0.924 | 4.327 | 0.800 | 4.998 | 0.693 | 5.773 |

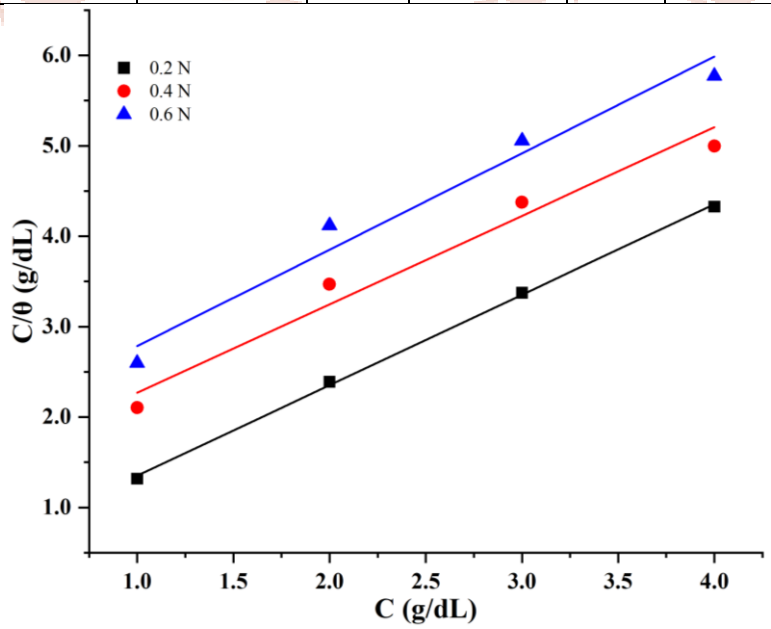


**Fig. 05: Langmuir adsorption isotherm for Al in different concentration HCl solution with AMLE at 301 ± 1 K.**

### 3.5 Thermodynamic parameter:

Thermodynamic analysis exposes that, the average ΔG°ads value of -12.35 kJ/mol indicates physisorption as the adsorption process of AMLE for Al and the process is characterized by an adsorption layer exhibiting electrostatic properties[39]. The positive ΔH°ads values indicate enhanced surface coverage and improved protection efficacy due to a higher energy barrier against corrosion[40]. Furthermore, the positive ΔS°ads values suggested that the corrosion process is entropically favourable[41] show in table 04.

It quantifies the rate of the reaction under specific conditions of temperature, concentration, pressure, etc. In the context of corrosion, it can be derived from the Arrhenius equation (20).

$$k=Ae^{-Eads/(RT)} \quad \ldots (20)$$

Where, A is the pre-exponential factor (frequency factor), Eads is the activation energy, R is the universal gas constant and T is the absolute temperature (in Kelvin).

To measure the rate constant for Al corrosion in present of a green inhibitor, experiments has been carried out using gravimetric method at different temperature. The collected experimental data have been analyzed to derive the rate constant, facilitating a comparison of corrosion rates without and with the inhibitor.

The half-life (t1/2) time required for the concentration of the reactant to reduce to half its initial value. In the context of corrosion inhibitors, it gives insight into the longevity and efficiency of the inhibitor in reducing corrosion rates. For a first-order reaction, it can be expressed as equation (21). As AMLE concentration increases, rate constant k was decreases as well as half-life increases shown in table 05. A low rate constant k value indicating a slower reaction rate in a longer half-life, its mean that AMLE is effective over an extended period[42].

$$t_{1/2} = \frac{0.693}{K} \quad \ldots (21)$$

**Table 04: Thermodynamic parameters of Al in 0.2 N HCl solution without and with of different inhibitor concentration of *AMLE*.**

| Inhibitor | Inhibitor concentration g/dL | ΔG°ads | | | | ΔH°ads | | ΔS°ads | |
|---|---|---|---|---|---|---|---|---|---|
| | | 313 K | 323 K | 333 K | Mean | 313 K | 323 K | 313 K | 323 K |
| **Blank** | 0.0 | - | - | - | - | 23.17 | 19.73 | - | - |
| ***AMLE*** | 1.0 | -11.34 | -12.23 | -13.48 | -12.35 | 47.00 | 45.87 | 0.110 | 0.099 |
| | 2.0 | | | | | 55.01 | 49.54 | 0.186 | 0.180 |
| | 3.0 | | | | | 52.97 | 58.30 | 0.212 | 0.191 |
| | 4.0 | | | | | 56.52 | 61.98 | 0.205 | 0.218 |

**Table 05: Kinetic data for the corrosion of Al in different concentration of HCl solution with AMLE.**

| Inhibitor | Inhibitor concentration g/dL | Acid Concentration (HCl) | | | | | |
|---|---|---|---|---|---|---|---|
| | | 0.2 N | | 0.4 N | | 0.6 N | |
| | | Rate constant ($k \times 10^{-3}$) ($day^{-1}$) | Half life ($t_{1/2}$) (day) | Rate constant ($k \times 10^{-3}$) ($day^{-1}$) | Half life ($t_{1/2}$) (day) | Rate constant ($k \times 10^{-3}$) ($day^{-1}$) | Half life ($t_{1/2}$) (day) |
| **Blank** | 0.0 | 71.36 | 9.71 | 120.86 | 5.73 | 180.47 | 3.84 |
| ***AMLE*** | 1.0 | 16.72 | 41.45 | 58.92 | 11.76 | 104.20 | 6.65 |
| | 2.0 | 11.29 | 61.39 | 51.58 | 13.44 | 91.71 | 7.56 |
| | 3.0 | 7.68 | 90.18 | 36.68 | 18.89 | 69.53 | 9.97 |
| | 4.0 | 5.23 | 132.47 | 23.08 | 30.03 | 52.35 | 13.24 |

**3.6 Potentiadynamic polarization method:**

The study employed potentiodynamic polarization measurements to assess the corrosion behavior of metals in acidic environments, focusing primarily on the influence of AMLE as corrosion inhibitors. The results demonstrated that AMLE significantly reduces corrosion activity when added to 0.2 N HCl solution containing for Al. The reduction in the icorr and largest shift in corrosion potential (Ecorr) is directly related to the concentration of AMLE increase, indicating that the inhibitor layer adsorbs and shields the Al surface from corrosion by HCl (Table 06). As the concentration of the extract without and with 4.0 g/dL, the polarization curves shifted towards less negative potentials and exhibited lower current densities, indicating good inhibition show in fig. 06. At high concentration of 4.0g/dL, the extract achieved 85.66% inhibition efficiency. The corrosion potential became less negative with higher extract concentrations and both anodic and cathodic Tafel decreased, reflecting a strong inhibitory effect primarily attributed to the adsorption of extract molecules on the Al surface worked as mixed type inhibitor.

**Table 06: Corrosion potential (Ecorr), Corrosion current density (iCorr), Tafel slopes (βa, βc), Corrosion rate (C.R.) and Inhibition efficiency (I.E. %) of Al in 0.2 N HCl.**

| Inhibitor | $-E_{corr}$ (V) | $i_{corr}$ ($\mu A/cm^2$) | Anodic ($+\beta_a$) V/dec | Cathodic ($-\beta_c$) V/dec | Corrosion rate (C.R.) (mpy) | Inhibition efficiency (I.E. %) |
|---|---|---|---|---|---|---|
| **Blank** | 0.738 | 143.00 | 0.37 | 14.85 | 244.9 | - |
| ***AMLE*** | 0.714 | 20.50 | 0.0965 | 3.42 | 35.9 | 85.66 |

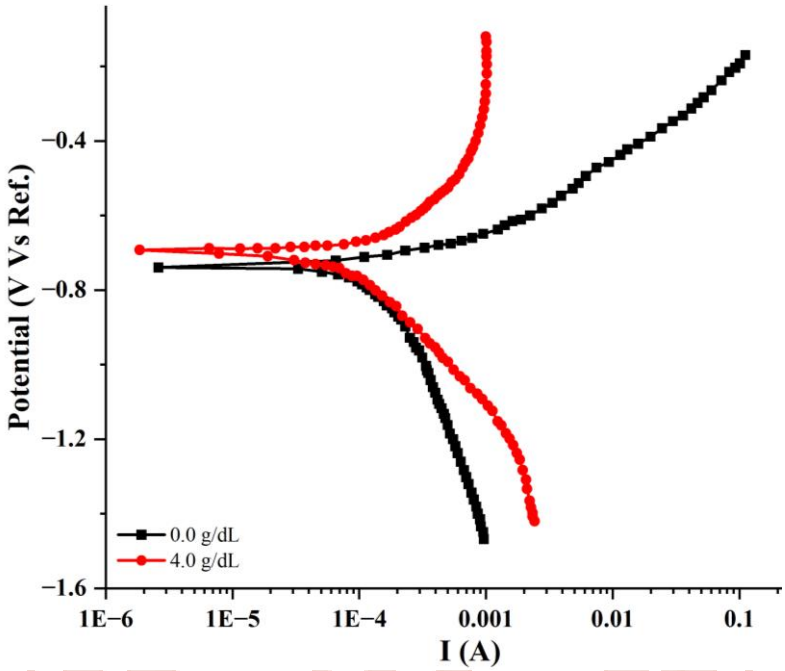


**Fig. 06: Tafel plot for Al in 0.2 N HCl solution without and with AMLE.**

### 3.7 Electrochemical impedance spectroscopy (EIS):

The corrosion behavior of Al in 0.2 N HCl was examined both in the absence and presence of AMLE using electrochemical impedance spectroscopy (EIS). Impedance data were analyzed to determine the charge transfer resistance (Rct) and double layer capacitance (Cdl), which were then used to calculate the inhibition efficiency. Fig. 07 illustrates the impedance spectra for Al immersed in 0.2 N HCl without and with 4.0 g/dL concentrations of AMLE. As shown in the figure 07, the impedance plots predominantly display a near semicircular shape, signifying that the corrosion process is primarily controlled by charge transfer and frequency dispersion of interfacial impedance which may result from surface heterogeneity due to roughness or other interfacial phenomena. The addition of AMLE increased Rct values in the HCl solution, indicating resistance to corrosion. Simultaneously, the double layer capacitance (Cdl) decreased significantly in the presence of the inhibitor, following a trend similar to the corrosion current density (icorr). This reduction in Cdl suggests that the inhibitor molecules adsorb onto the metal surface in acidic conditions. At higher inhibitor concentrations increased Rct values, correlating with improved inhibition efficiency. Rct recorded was 612.1 $\Omega cm^2$ with high Cdl 26.01 nF/cm2 without inhibitor concentration. Rct recorded was 4121.8 $\Omega cm^2$, with a minimum Cdl of 3.86 $nF/cm^2$ at an optimal concentration of 4.0 g/dL, found 85.15% inhibition efficiency. These findings are consistent with results obtained from non-electrochemical techniques such as gravimetric analysis as well as electrochemical approaches like potentiodynamic polarization.

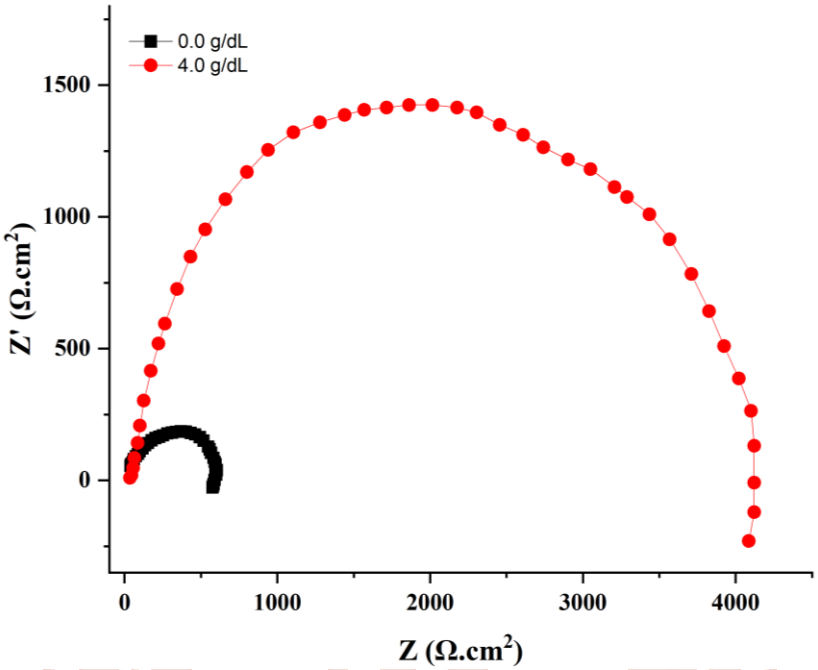


**Fig. 07: Nyquist plot for Al in 0.2 N HCl without and with *AMLE*.**

### 3.8 Surface and elements composition analysis:

#### 3.8.1 Scanning Electron Microscope (SEM):

Surface analysis of the Al specimen was conducted utilizing a scanning electron microscope (SEM) at a magnification of 1000X. The specimens were immersed in 0.2 N HCl solution for a duration of 24 hours, both without and with the addition of the 4.0g/dL concentration of AMLE. After the immersion, the samples were removed, dried and stored in a desiccator. SEM analysis of plain Al surface, Al immersed in HCl and Al immersed in HCl with AMLE shown in figure 08(a), 08(b) and 08(c) respectively. SEM observations confirmed the formation of a protective film on the surface of the Al. It was observed that a layer forms as a result of AMLE molecules adsorbing onto the surface, creating a coating layer. This result suggested that AMLE as a highly efficient corrosion inhibitor by adsorbing onto the Al surface in a 0.2 N HCl solution[6,7].

**08(a) Plain Al surface**

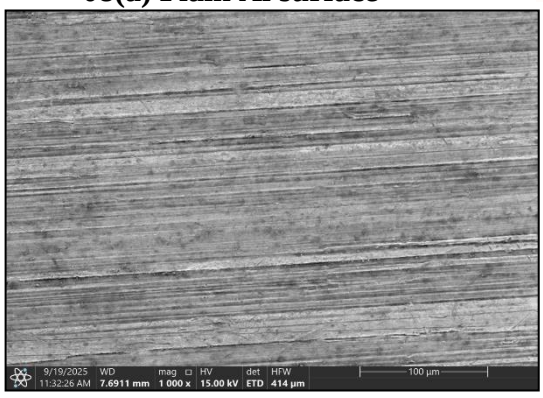

**08(b) Blank**

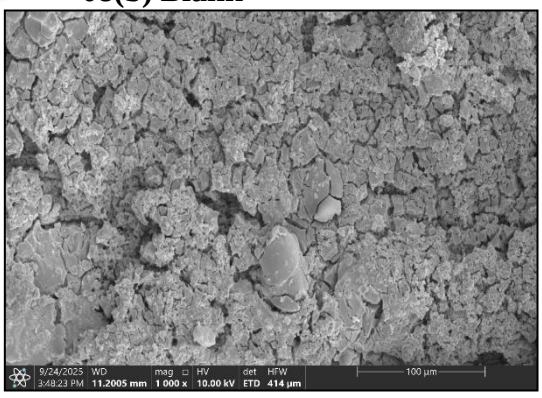

**08(c) with *AMLE***

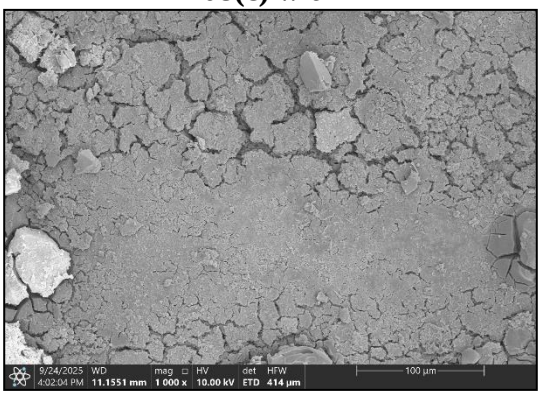

**Fig. 08: SEM images of plain Al and Al in 0.2 N HCl without and with *AMLE*.**

### 3.8.2 Energy-Dispersive X-Ray Spectroscopy (EDX):

The EDX spectra shown in figure 09(a) to 09(c) offer insights into the location and strength of the peaks, aiding in the identification of the elements and their approximate quantities. According to Table 07, the Al samples treated with AMLE molecules markedly inhibit the development of aluminum oxide, leading to decreased oxygen (O) levels on the aluminum surface while the proportion of aluminum (Al) increases, these compounds serve as effective protectants against aluminum corrosion. This suggests that AMLE molecules produced protective layer that facilitated the development of a protective aluminum layer[6].

**Table 07: EDX spectra of plain Al and immersed Al in 0.2 N HCl without and with *AMLE*.**

| System | Percentage (%) of atomic weight | | | | | | | | |
|---|---|---|---|---|---|---|---|---|---|
| | Al | O | Cl | Br | Bi | P | Ca | Mg | N |
| **Plain Al** | 92.6 | 2.2 | 0.0 | 5.2 | 0.0 | 0.0 | 0.0 | 0.0 | 0.0 |
| **Blank** | 30.8 | 44.6 | 14.5 | 4.9 | 5.2 | 0.0 | 0.0 | 0.0 | 0.0 |
| **AMLE** | 39.2 | 38.8 | 3.5 | 0.0 | 0.0 | 9.5 | 8.4 | 0.5 | 0.1 |

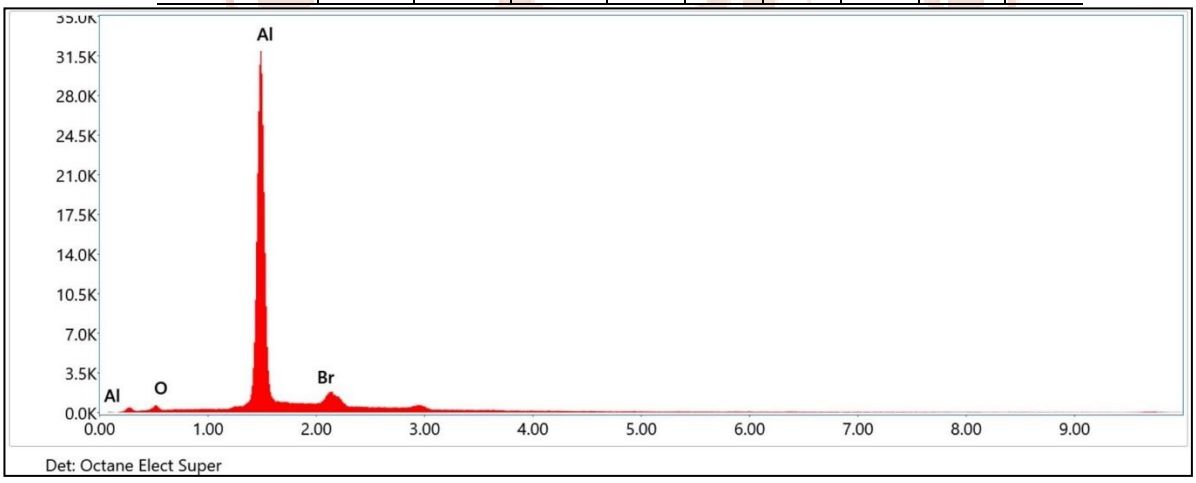


09(a) Plain Acid

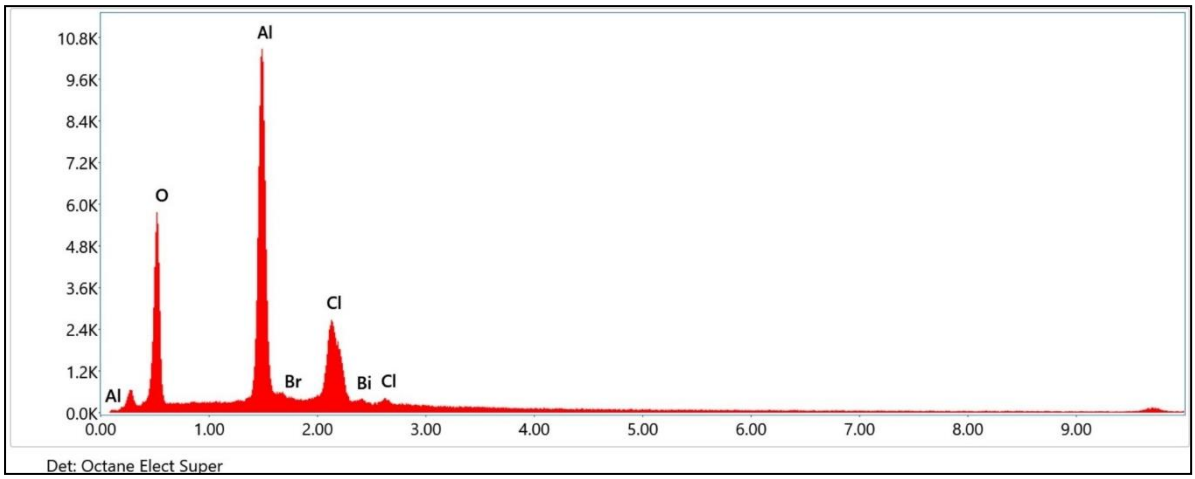


09(b) Blank

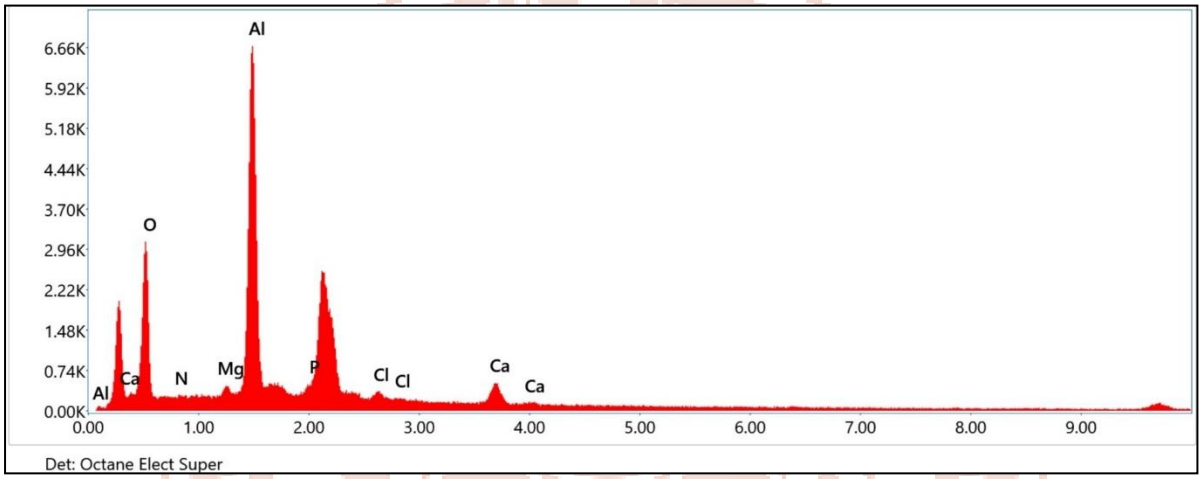


09(c) with *AMLE*

**Fig. 09: EDX spectrums of plain Al metal, Al in 0.2 N HCl without and with of *AMLE*.**

**3.9 Density functional theory:**

The DFT calculations has been provide insights into the electronic properties of phytochemical present in AMLE, allowing for the prediction of their inhibition reactivity and interaction with the Al surface. In this study, DFT study employed to show the contribution of different types of isolated molecules of AMLE. The geometric optimized structure (neutral) of molecule orbitals (LUMO and HOMO), Mulliken charge distributed structure and Total electron density shown in fig. 10 and Table 08 shows value without and with solvent of energy gap (ΔE), Absolute electronegativity (χ), Global hardness (η), Global softness (σ) and Electrophilicity index (ω), electron accepting power (ω+), electron accepting power (ω-), nucleophilicity index (ε), electron density (ΔN) and dipole moment (μ) for Aegeline (A) and Qurecetin (B) molecules.

In aqueous solution, the energy gap calculated as ΔE (4.56, 4.44, 4.49 and 4.46 eV) smaller ΔE value indicates that the both phytochemical constituents has a higher potential to donate electrons, facilitating strong interaction with the metal surface and increasing its

inhibition efficiency[43]. As per frontier molecular theory, the inhibitor molecules with higher HOMO energies were to have a higher tendency to donate electrons to the Al surface, leading to stronger interactions and better inhibition. Conversely, molecules with lower LUMO energies are expected to be better electron acceptors from the metal surface[44]. The energies associated with the HOMO and LUMO levels provide insight into the stability of the inhibitor molecule structure during the corrosion process. The calculated energy values (eV) in water as solvent for HOMO and LUMO levels can be summarized as show in table 08. The HOMO-LUMO gap provides crucial information regarding the reactivity of inhibitor molecules. A smaller energy gap typically indicates a greater tendency for the compound to donate electrons, leading to increased nucleophilicity and enhanced inhibition properties. Absolute Electronegativity ($\chi$) can be related to the tendency of the molecules to attract electrons. Higher electronegativity (3.94, 4.05, 3.95, 4.11 eV) implies a stronger ability to stabilize the cation in an electrochemical reaction. The positive value (2.28, 2.22, 2.25, 2.23 eV) of global hardness ($\eta$) indicates more stable molecules that are less reactive[45].

The positive value (3.40, 3.70, 3.46 and 3.79 eV) of electrophilicity index ($\omega$) indicates a molecule acquire electrons. A higher value suggests a stronger electrophile, which can enhance the ability of the molecule to act as an inhibitor. The ability of phytochemicals to accept or donate electric charge has been determine from positive value $\omega+$ (1.71, 1.95, 1.77 and 2.01 eV) and $\omega-$ (5.65, 6.00, 5.72 and 6.12 eV), of electron accepting ($\omega+$) and donating ($\omega-$) power to understanding in the corrosion process. A smaller value of back donation $\Delta E$ (-0.57, -0.55, -0.56 and -0.55) eV indicates the AMLE has a higher potential to donate electrons. Inhibitor molecules with higher value (3.17, 5.04, 5.41 and 6.91 eV) of dipole moments ($\mu$) can expected to have stronger electrostatic interactions with the charged Al surface[46]. The calculated Mulliken charge distribution to identify the preferred adsorption sites of the AMLE molecules. Atoms with higher negative charges are expected to interact strongly with the Al surface, leading to the establishment of coordinate bonds. This quantum study indicates that inhibitor employed has maximum adsorption on the surface of metal to form a protection layer[47,48].

**Table 08: The quantum study information for the neutral form of A and B inhibitor molecules without and with solvent.**

| Inhibitor | Solvent | HOMO (ev) | LUMO (ev) | I (ev) | A (ev) | ΔE (ev) | χ (ev) | γ or η (ev) | σ (ev) | ω (ev) | ω+ (ev) | ω- (ev) | ε (ev) | ΔN (ev) | ΔE Back donation (ev) | μ (debye) |
|---|---|---|---|---|---|---|---|---|---|---|---|---|---|---|---|---|
| A | Gas | -6.22 | -1.66 | 6.22 | 1.66 | 4.56 | 3.94 | 2.28 | 0.44 | 3.40 | 1.71 | 5.65 | 0.29 | 0.51 | -0.57 | 3.17 |
| | Water | -6.28 | -1.83 | 6.27 | 1.83 | 4.44 | 4.05 | 2.22 | 0.45 | 3.70 | 1.95 | 6.00 | 0.27 | 0.55 | -0.55 | 5.04 |
| B | Gas | -6.19 | -1.70 | 6.19 | 1.70 | 4.49 | 3.95 | 2.25 | 0.45 | 3.46 | 1.77 | 5.72 | 0.29 | 0.52 | -0.56 | 5.41 |
| | Water | -6.34 | -1.88 | 6.34 | 1.88 | 4.46 | 4.11 | 2.23 | 0.45 | 3.79 | 2.01 | 6.12 | 0.26 | 0.56 | -0.55 | 6.91 |

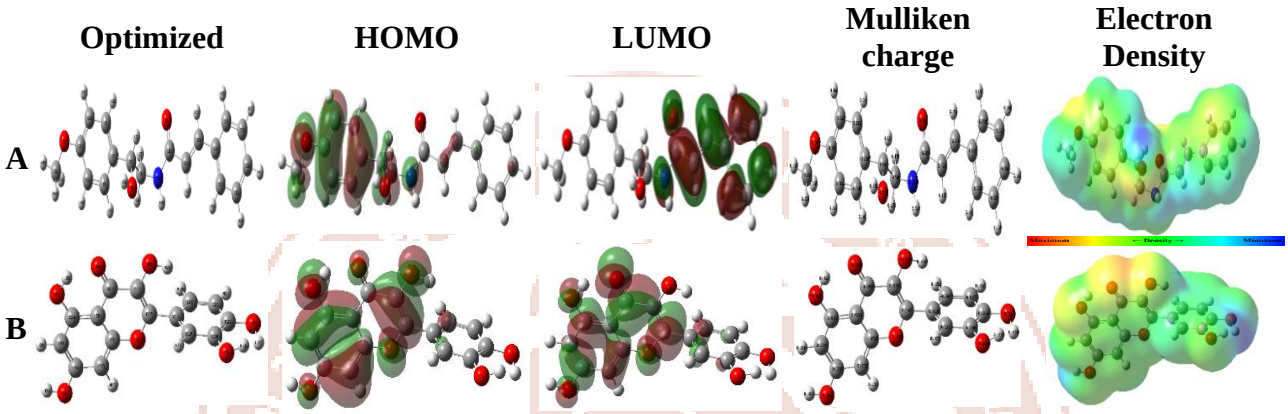


**Fig. 10: Optimized structure, HOMO - LUMO structure, Mulliken charge structure and Total electron density for A and B inhibitor molecules.**

### 3.10 Molecular Dynamics (MD) Simulation:

The Molecular dynamic simulation was performed to investigate the dynamic behaviour of the AMLE inhibitor deformation, adsorption and total energies on the Aluminium metal surface in presence of hydrochloric acid solution (aqueous media) interface. The total energy (kcal/mol) for substrate and AMLE adding molecular energies from rigid adsorption as measure kcal/mol by dEads/dAl, obtain the energy during the adsorbate separate from the adsorbent substrate (Table 09). The substrate energy is set to 0 for reference. The dEads/dAl values for AMLE molecules are higher than from water molecules. It shows that AMLE is adsorbed stronger interaction than water molecules[49].

The adsorption energy is total of the rigid adsorption energy and the deformation energy of the adsorbate compounds which are study in kcal/mol by dEads/dAl show in table 09. The value of rigid adsorption energy show the basic energetic interaction between the adsorbate and the adsorbent. The simulations will reveal the adsorption mode and orientation of the inhibitor molecules on the Al surface. The water molecules and chloride ions interact with the Al surface and with the inhibitors. The flat adsorption mode is generally associated with a more effective inhibitor and is usually preferred[50]. The inhibitors exhibit electron donating capacity and their reaction involve the adsorption of inhibitor molecule on the metal surface

via lone pair electron of nitrogen and oxygen atom. This study result expected that inhibitor molecule produce stable protective adsorption layer on surface of metal (Fig. 11). The adsorbed inhibitor molecules block the active sites on the Al surface, preventing the interaction of the metal with the corrosive entities like chloride ions retarding the corrosion process.

**Table 09: Adsorption data derived from the adsorption locator for inhibitor molecules of *AMLE*.**

| Inhibitor Molecule | Total energy (kcal/mol) | Adsorption energy (kcal/mol) | Rigid adsorption energy (kcal/mol) | Deformation energy (kcal/mol) | $H3O^+$ $dE_{ad}/dN_i$ (kcal/mol) | $Cl^-$ $dE_{ad}/dN_i$ (kcal/mol) | $H_2O$ $dE_{ad}/dN_i$ (kcal/mol) | Inhibitor $dE_{ad}/dN_i$ (kcal/mol) |
|---|---|---|---|---|---|---|---|---|
| **Aegeline** | -3635.14 | -3800.99 | -3811.81 | -10.82 | -158.43 | -153.24 | -13.07 | -121.05 |
| **Quercetine** | -3563.42 | -3781.44 | -3764.03 | -17.40 | -159.43 | -147.78 | -14.55 | -112.42 |

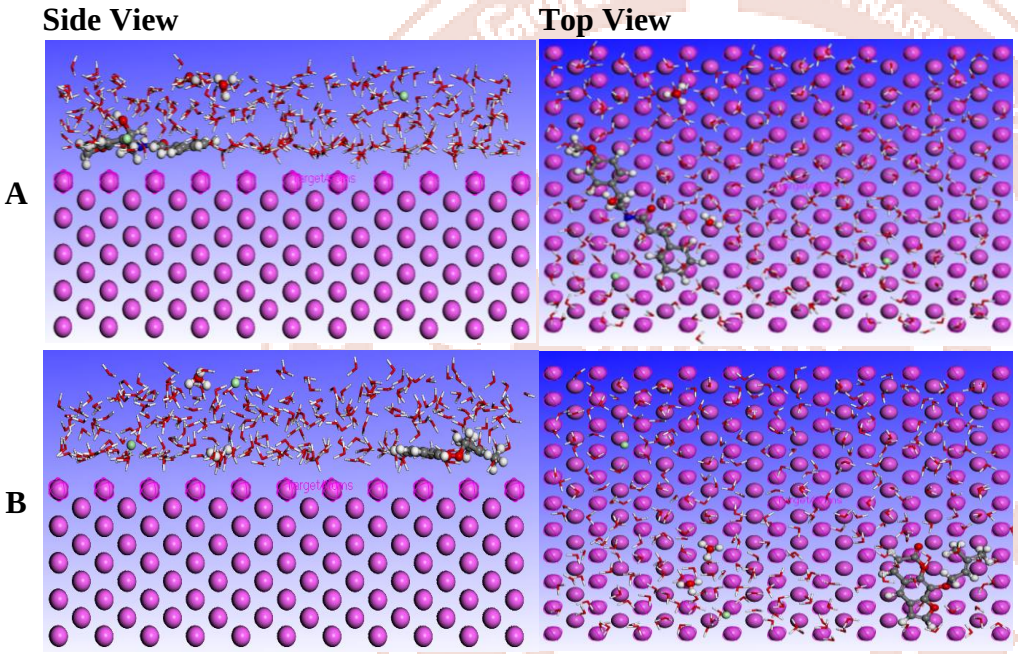


**Fig. 11: The most stable configuration for adsorption of A and B inhibitor molecules on Al (110) surface.**

## 4. Inhibition Mechanism:

The inhibition mechanism of Aegle marmelos leaves water extract against Al metal corrosion in hydrochloric acid involves a combination of physical adsorption and chemical interactions that form a protective barrier on the metal surface. Several studies have shown that organic compounds, particularly those containing functional groups like hydroxyl or amine, can create a protective barrier[51]. The aqueous extract introduced into the corrosive medium, its bioactive compounds such as flavonoids, phenolics compounds, tannins and alkaloids interact with the Al surface. These organic molecules contain heteroatoms like oxygen and nitrogen and functional group like -OH and -OCH3 which possess lone pairs of electrons

capable of donating to vacant d-orbitals of Al atoms. This electron donation facilitates the adsorption of inhibitor molecules onto the metal surface, creating a passive film that impedes the ingress of corrosive species like H+ and Cl- ions[52]. The adsorption process is primarily governed by physisorption, characterized by electrostatic interactions between the charged or polar functional groups in the extract and the metal surface. The formation of this adsorbed film reduces the active sites available for corrosion reactions, thereby decreasing the rate of metal dissolution. Bioactive compounds of leaves undergo chemisorption, forming coordinate bonds with surface Al atoms, which further stabilizes the protective layer. This adsorption process is crucial, as it creates a protecting barrier that avoids corrosive agents such as $H^+$ ions in acidic solutions from directly contacting the Al substrate. The researchers suggest that the inhibitive action of inhibitor molecules in HCl solution attributed to the adsorption of inhibitor molecules onto the metal surface, resulting in the formation of a protective layer[53, 54]. The presence of phenolic compounds and tannins enhances the film's integrity and adhesion, providing a long-lasting barrier against acid attack on the metal surface[55]. The extract's constituents also neutralize free chloride ions or reduce the acid's aggressiveness, contributing to the corrosion inhibition process. Overall, the inhibition mechanism involves the spontaneous adsorption of organic molecules from AMLE onto aluminium forming a protective, adherent layer that prevents direct contact between Al and the aggressive HCl medium, thus effectively reducing corrosion rates.

## 5. Conclusion:

- The *AMLE* was found to have the highest inhibition efficiency up to 92.43% in 0.2 N HCl solution at 301 ± 1 K.
- At the constant acid concentration the inhibition efficiency increases as the inhibitor concentration increases, but decreases with increase in temperature and at constant inhibitor concentration the inhibition efficiency decreases with increase acid concentration.
- The corrosion process is hindered AMLE due to adsorption on Al surface, following Langmuir adsorption isotherm.
- The negative free energy of adsorption ($\Delta G^o_a$) value suggest that a strong and spontaneous nature of *AMLE* adsorption on Al surface.
- EIS findings demonstrate that AMLE acts as a highly effective corrosion inhibitor by enhancing charge transfer resistance and establishing a durable protective film on Al surface.

- The SEM and EDX analyses verified the development of a protective coating on the Al surface, substantially mitigating corrosion in HCl solution and highlighting the inhibitor's effectiveness.
- The DFT calculations indicted the inhibitor molecules has most electron donating-accepting susceptibility via π-π stacking and hydrogen bonding interactions.
- The MD simulation results shows that the phytochemical compound significant capacity to interaction and adsorption on Al surface.
- The *AMLE* acts as an eco-friendly inhibitor for Aluminium corrosion in acidic environment.

**Acknowledgement:**
The authors are grateful to the Department of Chemistry, C. B. Patel Computer College & J. N. M. Patel Science College, Surat for providing laboratory facilities.

## References:

1. Rosliza R., Wan Nik W. B. and Senin H. B., The effect of inhibitor on the corrosion of aluminium alloys in acidic solutions, Mater. Chem. Phys., **107**, 281-288 (2008).
2. Xhanari K. and Finsgar M., Organic corrosion inhibitors for aluminium and its alloys in acid solutions: A Review. RSC Adv. **6**, 62833-62857 (2016).
3. Patel J., Charmi L., Joshi M. and Desai D., Graphene/Epoxy based barrier coatings for corrosion protection: A Review, JETIR, **11**(2) (2024).
4. Erfan K. and Mardali Y., A study of pomegranate peel extract effect on corrosion inhibition performance on aluminum in $HNO_3$ solution, Colloids and Surfaces A: Physicochemical and Engineering Aspects, **694**, 134080 (2024).
5. Ifeyinwa C. E. , Chukwuebuka E. M., Charity N. N., Chinedu F. A. and Chigoziri N. N., Musa paradisiaca stem sap extract as corrosion inhibitor for aluminum protection in acidic environment, Zastita materijala, **65** (2025).
6. Fouda A. S., Etaiw S. H. and El-Hussieny E. S., Yellow Oleander Extract as Green Sustainable Corrosion Inhibitor for Aluminum in Hydrochloric Acid Solution, Egypt. J. Chem. **68** (2), 493-505 (2025).
7. Glory O. J., Okeke P. I., Appolinus E., Blessing E., Sunday O., Amanze K. and Nleonu E. C., Green corrosion inhibition of aluminium in acidic environment using Hibiscus sabdariffa leaf extracts, Preprints-Web of Science, (2025).
8. EL-Haddad M.N. and Fouda A. S., Investigating Xanthium spinosum extract as an eco-friendly corrosion inhibitor for Aluminium in acidic environments: A green approach to metal protection, Results in Chemistry, **14**, 102136 (2025).

9. Boughoues Y., Benamira M., Messaadia L. and Ribouh N., Adsorption and corrosion inhibition performance of some environmental friendly organic inhibitors for mild steel in HCl solution via experimental and theoretical study, Colloids Surfaces A Physicochem Eng Asp, **593**,124610 (2020).
10. Mounia S., Mina B., Aissa C., Youssef L. and Ala A., Aqueous extract of Punica granatum fruit peel as an eco-friendly corrosion inhibitor for aluminium alloy in acidic medium, Journal of Bio- and Tribo-Corrosion, **8**, 54 (2022).
11. Desai S. A., Prajapati N. I. and Vashi R. T., Inhibitory Effects of Delonix regia (Gulmohor) extract on corrosion of aluminium in Hydrochloric Acid, JETIR, **5**(10), 136-145 (2018).
12. Abu Orabi F. M., Abu-Orabi S. T., Fodeh O. A., Algethami F. K., Rawashdeh A. M. M., Bataineh T. T., Al-Mazaideh G. M. and Al-Qudah M. A., Ajuga orientalis L. Extract as a Green Corrosion Inhibitor of Aluminum in an Acidic Solution: An Experimental and DFT Study, Metals, **14**(11), 1227 (2024).
13. Verma C., Quraishi M. A., Ebenso E. and Bahadur I., A green and sustainable approach for mild steel acidic corrosion inhibition using leaves extract: experimental and DFT Studies, J. of Bio- and Tribo-Corrosion, **4**, 33 (2018).
14. Bansal S. and Bansal G., Analytical methods for standardization of Aegle marmelos: A review, J. Pharm. Educ. Res., **2**(2) (2011).
15. Yadav N. P. and Chanotia C. S., Phytochemical and pharmacological properties of Aegle marmelos linn. Alternative medicine / Nutraceuticals, The pharma review (2009).
16. Jhajhria A. and Kumar K., Tremendous pharmacological values of Aegle marmelos, Int. J. Pharm. Sci. Rev. Res., **36**(2) (2016).
17. Monika S., Thirumal M. and Kumar P. R., Phytochemical and biological review of Aegle marmelos Linn, Future Sci. (2023).
18. Bhardwaj N., Prasad D. and Haldhar R., Study of the Aegle marmelos as a Green Corrosion Inhibitor for Mild steel in acidic medium, J. of Bio- and Tribo-Corrosion, **4 (**61) (2018).
19. Logan S. R., The origin and status of the Arrhenius equation, J. of chemical education, **59**(4), (1982).
20. Oguzie E. E., Evaluation of the inhibitive effect of some plant extracts on the acid corrosion of mild steel, Corros. Sci., **50**(11), 2993 (2008).
21. Prajapati N. I., Vashi R. T. and Desai S. A., Fennel (foeniculum vulgare mill) seeds extract as green inhibitor for aluminium corrosion in HCl acid solution: thermodynamic, adsorption and kinetic stud, EIBPS, **7**(6), 421-428 (2020).

22. Thomson R. H., Naturally occurring quinones, third ed., Academic Press, London, New York, **74**, (1971).
23. Perez P., Contreras R., Vela A. and Tapia O., Relationship between the electronic chemical potential and proton transfer barriers, Chem. Phys. Lett., **269**, 419-427 (1997).
24. Geerlings P., De Proft F. and Langenaeker W., Conceptual density functional theory, Chem. Rev., **103**, 1793–1874 (2003).
25. Sadik K., El hamdani N., Byadi S. and Hachim M., Quantum and dynamic investigations of Complex iron- alkaloid-extract Cytisine derivatives of Retama monosperma (L.) Boiss. Seeds as eco-friendly inhibitors for Mild steel corrosion in 1M HCl, J. Mol. Struct., 1244, 130921 (2021).
26. Husaini M., Yunusa U., Ibrahim H. A., Usman B., and Ibrahim M. B., Corrosion inhibition of aluminum in phosphoric acid solution using glutaraldehyde as inhibitor, Algerian J. of Chemical Engineering, **1**(13-21) (2020).
27. Neese F., Wennmohs F., Becker U. and Riplinger C., The ORCA quantum chemistry Program Package, J. Chem. Phys., **152**(22), 224108 (2020).
28. Franco M. and Gázquez J., The electronegativities of pauling and mulliken in density functional theory, The J. of Physical Chemistry, (2019).
29. Hanane H., Tahar D., Al-Noaimi M., Saifi I., Daoud D. and Salah C., Electrochemical and quantum chemical studies of some azomethine compounds as corrosion inhibitors for mild steel in 1 M hydrochloric acid, Corrosion Science, **88**, 234-245, (2014).
30. Abd El Wanees S., Kamel M. M., Ibrahim M., Rashwan S. M., Atef Y. and Abd Elsadek M. G., Corrosion inhibition and synergistic effect of ionic liquids and iodide ions on the corrosion of C-steel in formation water associated with crude oil, J. of Umm Al-Qura University for Applied Sciences, **10**, 107-119 (2024).
31. Metropolis N., Rosenbluth A. W., Rosenbluth M. N. and Teller A. H., Equation of state calculations by fast computing machines, J. Chem. Phys., **21**, 1087-1092 (1953).
32. Konn C., Charlou J. L., Holm N. G. and Mousis O., The production of methane, hydrogen, and organic compounds in ultramafic-hosted hydrothermal vents of the mid-atlantic ridge, Astrobiology, **15**, 381-399 (2015).
33. Deyab M. A., Egyptian licorice extract as a green corrosion inhibitor for copper in hydrochloric acid solution, J. Ind. and Eng. Chem., **22**, 384-389 (2015).
34. Jain T. and Chowdhary R., Electrochemical behavior of aluminium in acidic media, Materials and Corrosion **57**(5), 422-426 (2006).

35. Vashi R. T. and Bhajiwala H. M., Inhibition of corrosion of zinc in ($HNO_3$ + HCl) acid mixture by aniline, J. Fundam. Appl. Sci., **7(2)**, 299-306 (2015).
36. Martinez J. S. and Matikos Hukovic M., A nonlinear kinetic model introduced for the corrosion inhibitive properties of some organic inhibitors, J. Appl. Electrochem., **33**, 1137-1147 (2003).
37. **Paul A. A., Kelechukwu B. O. and Uchenna S. M., Adsorption and thermodynamic studies of the corrosion inhibition effect of Rosmarinus officinalis L. leaves on aluminium alloy in 0.25 M HCl and effect of an external magnetic field,** Int. J. Phys. Sci.**, 16 (2), 79-95 (2021).**
38. Adejo S., Uzah T. and Akuhwa J., Adsorption isotherm modeling in corrosion inhibition studies, Corrosion Engineering Recent Breakthroughs and Innovative Solution, (2024).
39. Donahue F. M. and Nobe K., Theory of organic corrosion inhibitors and linear free energy relationship, J. Electrochem. Soc., **112**, 886-891 (1965).
40. Ansari K. R., Yadav D. K., Ebenso E. E. and Quraishi M. A., Novel and effective pyridyl substituted 1, 2 ,4-triazole as corrosion inhibitor for mild steel in acid solution, Int. J. Electrochem. Sci., **7(5)**, 4780-4799 (2012).
41. Issa R. M., El-Sonbati A. Z., El-Bindary A. A. and Kera H. M., Polymer complexes XXXIV potentiometric and thermodynamic studies of monomeric and polymeric complexes containing 2-acrylamidosulphadiazine, Eur. Polym. J., **38**(3), 561-566 (2002).
42. Talati J. D. and Modi R. M., Inhibition of corrosion of aluminium-copper alloy in NaOH, Trans. SAEST., **11**, 259 (1986).
43. Arukalam I. O., Durability and synergistic effects of KI on the acid corrosion inhibition of mild steel by hydroxypropyl methylcellulose, Carbohydr Polym., **112**, 291-299 (2014).
44. Singh P., Srivastava V. and Quraishi M. A., Novel quinolone derivatives as green corrosion inhibitors for mild steel in acidic medium: electrochemical, SEM, AFM and XPS studies, J. of Molecular Liquids, **216**, 164-173 (2016).
45. Ebenso E. E., Isabirye D. A. and Eddy N. O., Adsorption and quantum chemical studies on the inhibition potentials of some thiosemicarbazides for the corrosion of mild steel in acidic medium, Int. J. Mol. Sci., **11**, 2473-2498 (2010).
46. Kokalj A. and Kovačević N., The consistent use of electrophilicity index and HSAB-based electron transfer and its associated change of energy parameters, Chem. Phys. Lett., **507**, 181-184 (2011).
47. Amitha Rani B. E. and Bharathi Bai J. B., Green inhibitors for corrosion protection of metals and alloys: an overview, Int. J. of Corrosion, **2012**, 380217 (2012).

48. Ime B. O., Digby M. and Zuhair G., Density functional theory (DFT) as a powerful tool for designing new organic corrosion inhibitors, part 1: an overview, Corrosion science, **99**(3), (2015).
49. Gadow H. S., Motawea M. M. and Elabbasy H. M., Investigation of myrrh extract as a new corrosion inhibitor for K-brass in 3.5% NaCl solution polluted by 16 ppm sulphide, RSC Advances, **7**(47), 29883-29898 (2017).
50. Mwadham M. K., Lutendo C. M., Muzaffer O., Faruk K., İlyas D., Ime B. O. and Eno E., Quantum chemical studies on the corrosion inhibition of mild steel by some triazoles and benzimidazole derivatives in acidic medium, Int. J. of Electrochemical Science, **7**(6)**,** 5035-5056 (2012).
51. Emori W., Zhang R. H. and Okafor P. C., Adsorption and corrosion inhibition performance of multiphytoconstituents from Dioscorea septemloba on carbon steel in acidic media: characterization, experimental and theoretical studies, Colloids and Surfaces A: Physicochemical and Engineering Aspects, **590** (2020).
52. Shyamala M. and Arulanantham A., Aegle marmelos as effective corrosion pickling inhibitor on mild steel in hydrochloric acid, Nature Environment and Pollution Technology, **8**(3), (2009).
53. Hijazi K. M., Abdel A. M., Younes G. O. and Habchi R., Comparative study of the effect of an acidic anion on the mild steel corrosion inhibition using Rhus coriaria plant extract and its quercetin component, Portugaliae Electrochimica Acta, **39**, 237-252 (2021).
54. Shyamala M. and Kasthuri P. K., A comparative study of the inhibitory effect of the extracts of Ocimum sanctum, Aeglemarmelos, Andsolanum trilobatum on the corrosion of mild steel in hydrochloric acid medium, Int. J. of Corrosion, **2011**, 1-11 (2011).
55. Pasupathy A., Nirmala S., Abirami G., Satish A. and Paul R., Inhibitive action of Aegle marmelos extract on the corrosion of zinc in 0.5N $H_2SO_4$ Medium, IJSRP, **4**(3), (2014).